Biochemistry and Biophysics Reports 10 (2017) 287–296

Contents lists available at ScienceDirect

Biochemistry and Biophysics Reports

journal homepage: www.elsevier.com/locate/bbrep

Behavioral study of selected microorganisms in an aqueous electrohydrodynamic liquid bridge

Astrid H. Paulitsch-Fuchs[a,b,*], Andrea Zsohár[a], Adam D. Wexler[a], Andrea Zauner[b], Clemens Kittinger[b], Joeri de Valença[a], Elmar C. Fuchs[a]

[a] Wetsus, European Centre of Excellence for Sustainable Water Technology, Leeuwarden, The Netherlands
[b] Institute of Hygiene, Microbiology and Environmental Medicine, Medical University of Graz, Graz, Austria

ARTICLE INFO

Keywords:
Floating water bridge
Electrohydrodynamic liquid bridging
Bacillus subtilis subtilis
Neochloris oleoabundans
Saccharomyces cerevisiae
THP-1 monocytes
Protonic Faraday cage

ABSTRACT

An aqueous electrohydrodynamic (EHD) floating liquid bridge is a unique environment for studying the influence of protonic currents ($mA\,cm^{-2}$) in strong DC electric fields ($kV\,cm^{-1}$) on the behavior of microorganisms. It forms in between two beakers filled with water when high-voltage is applied to these beakers. We recently discovered that exposure to this bridge has a stimulating effect on *Escherichia coli.*. In this work we show that the survival is due to a natural Faraday cage effect of the cell wall of these microorganisms using a simple 2D model. We further confirm this hypothesis by measuring and simulating the behavior of *Bacillus subtilis subtilis*, *Neochloris oleoabundans, Saccharomyces cerevisiae* and THP-1 monocytes. Their behavior matches the predictions of the model: cells without a natural Faraday cage like algae and monocytes are mostly killed and weakened, whereas yeast and *Bacillus subtilis subtilis* survive. The effect of the natural Faraday cage is twofold: First, it diverts the current from passing through the cell (and thereby killing it); secondly, because it is protonic it maintains the osmotic pressure in the cell wall, thereby mitigating cytolysis which would normally occur due to the low osmotic pressure of the surrounding medium. The method presented provides the basis for selective disinfection of solutions containing different microorganisms.

1. Introduction

1.1. Background

The floating water bridge is a special case of an electrohydrodynamic (EHD) liquid bridge and constitutes an intriguing phenomenon that occurs when a high ($\sim kV\,cm^{-1}$) potential difference is applied between two beakers of pure water. Induced by the field, the water jumps to the edges of the beakers and creates a free hanging string through air connecting the two beakers. In spite of its ease of generation, the physical mechanism behind the formation of an EHD bridge and its relation to the microscopic properties of water are not completely understood. The discovery of the water bridge phenomenon goes back to the 19th century, when in 1893 Sir William Armstrong reported the discovery of this phenomenon [1]. In contrast to similar effects like electrowetting [2] or the Sumoto effect [3] the water bridge was forgotten until its recent rediscovery [4,5]. At the macroscopic level electrohydrodynamics discussions of the Maxwell stress tensor [6] are sufficient to provide an explanation of the gross features of the bridge. Under these scenarios the electric field induces a negative pressure which draws liquid into the bridge and also accelerates suspended liquid elements against gravity, essentially being a form of electrostriction. Formal relationships between the physical fluid parameters, electric field intensity, and experimental configuration have been worked out by Marín and Lohse [7]. Aerov [8] on the other hand proposes a model where surface tension is responsible for holding the bridge against the gravity, whereas the electric field assures stability with respect to decomposition into droplets (the Rayleigh-Plateau instability). Woisetschläger et al. [9] present a macroscopic theory based on the works of Widom et al. [6] and Marín and Lohse [7]. They show theoretically and experimentally that floating liquid bridges are not water intrinsic, any liquid with dielectric permittivity, low electric conductivity, and a permanent molecular dipole moment can be used to create one. Thus bridging can be reproduced with other liquids that possess properties similar to water [9] such as methanol [10], ethanol, propanol [11] or glycerol [7]. An interesting question is whether the macroscopic phenomenon of EHD bridge formation is associated with detectable changes of water on the molecular scale. The molecular-scale properties of an aqueous EHD bridge have been studied with Raman-, neutron- and inelastic UV scattering as well as interferometry [12–15].

* Corresponding author at: Wetsus, European Centre of Excellence for Sustainable Water Technology, Leeuwarden, The Netherlands.
E-mail address: astrid.paulitsch-fuchs@wetsus.nl (A.H. Paulitsch-Fuchs).

http://dx.doi.org/10.1016/j.bbrep.2017.04.015
Received 14 November 2016; Received in revised form 9 March 2017; Accepted 22 April 2017
Available online 28 April 2017

Molecular dynamics simulations show effects of electric fields on water structure [16,17] or even increase dissociation [18,19], but these calculations concerned electric fields that are ~1000 times higher than those needed to form an EHD bridge. Ultrafast IR pump/probe spectroscopy showed that the OH relaxation of an HDO molecule in D_2O lies in the phase transition range of bulk water whereas the thermalization dynamics following this relaxation are considerably slower [20]. The electrochemistry of the system has been thoroughly investigated [21] revealing the bridge to be a protonic semi-conductor, with protons being the main charge carrier. Generated in the anolyte by electrolysis they are transported to the catholyte through the bridge. In the bridge the protons are more mobile than in the bulk [22] and their transport causes a non-thermic IR emission [23]. Details about how to safely build and run an EHD bridge set-up are described by Wexler et al. [24].

A number of studies were undertaken about the effects of electric fields on living cells: electrophoresis and dielectrophoresis for manipulating or sorting cells (e.g. reviews on this topic [25–28]:), electroporation of cells [29–32], and sterilization of liquids and food by pulsed electric field [33–36]. It should be pointed out that none of these methods are comparable to the study presented in this work. In the quoted methods the effect of the electric field on the cell and protonic currents are either negligible (sorting cells), or the field and associated electronic currents are destructive on purpose (electroporation and disinfection). For sterilization normally pulsed fields are applied (e.g [36].) involving discharges and associated chemical reactions (for instance radical and peroxide formation) due to the injected electrons. In an EHD liquid bridge, there are no discharges, the field is constant (not pulsed), and a protonic current is present. In addition, the bridge bases are locations of strong field gradients [9,37]. A Raman investigation [38] has shown that such gradients establish an excited subpopulation of vibrational oscillators far from thermal equilibrium. Hindered rotational freedom due to electric field pinning of molecular dipoles [23,38] retards the heat flow and generates a chemical potential gradient responsible for observable changes in the refractive index and temperature, exhibiting local non-equilibrium thermodynamic transient states critical to biochemical processes. A comparable situation is thus present across the membrane of living cells [39]. In general it is therefore possible to view the bridge as a macroscopic simulation of water in cell membranes.

1.2. Motivation

The behavior of *Escherichia coli* top10 and bioluminescent *Escherichia coli* YMC10 with a *Vibrio fischeri* gene plasmid in an EHD bridge set-up was recently investigated [37] and yielded unexpected results: Although the environment is supposedly hostile for the bacteria due to the low osmotic pressure and the strong electric field, most of the *E. coli* cells survived the transport through the bridge and showed increased activity (more intense luminescence and higher optical density (OD), respectively) after 24 h. In order to explain this behavior a hypothesis was presented: Only the strongest of the bacteria survive, therefore bacterial activity is increased after exposure. In the present work this hypothesis is further explored by conducting experiments with additional microorganisms and simple 2D model calculations thereof. As result a cellular mechanism responsible for the survival is presented: If the organisms possess a natural protonic Faraday cage – a highly proton-conductive layer – the current does not pass through the cell but around, and the local osmotic pressure is maintained by constant resupply of protons. If such a layer is absent, most of the organisms are weakened and/or die. This distinction provides the basis for a number of applications targeted at the distinction of microorganisms based on their electric properties, like, for example, selective disinfection or stimulation.

2. Methods and experimental set-up

2.1. EHD experiments

This study comprises experiments with the gram positive bacteria *Bacillus subtilis subtilis*, the yeast *Saccharomyces cerevisiae*, and the algae *Neochloris oleoabundans*. The bacteria and yeast cultures were grown in TSB medium (30 g/L Caso bouillon (TSB) powder; pH 7.3), for the algae culture a medium developed specifically for *N. oleoabundans* was used (24.5 g/L NaCl, 9.8 g/L $MgCl_2{\cdot}6H_2O$, 0.53 g/L $CaCl_2{\cdot}2H_2O$, 3.2 g/L Na_2SO_4, 0.85 g/L K_2SO_4, 2.72 g/L $NaNO_3$, 2.5 mL/L EDTA ferric sodium solid, 2.5 mL/L micronutrients, 1 mL/L vitamins, 5 mL/L phosphate, 10 mL/L bicarbonate; pH 7). For the agar plates 15 g/L agar powder was added to the liquid medium. All the cultures were incubated at 25 °C.

All tools (beakers, electrodes, cylinder, 15 mL Greiner tubes, Eppendorf tubes) and liquids (Milli-Q water, 5% glycerol solution, PBS buffer solution) were autoclaved (25 min, 121 °C) before the experiments. 15 mL Greiner tubes were filled with 4.5 mL 2xTSB or 2x algae medium. The cells were harvested from an overnight culture, in the algae's case from a 7 days culture. The 2 mL Eppendorf tubes were filled with the solution and centrifuged (3 min, 13.2 rpm); then the cells were washed with 5% glycerol solution and centrifuged again. The cell density of the stock solution was adjusted to McFarland 1 (~$3{\cdot}10^8$ cells/mL for bacteria, ~$1{\cdot}10^7$ cells/mL for yeasts) value. The solution and the Milli-Q water were kept on ice until the experiment in order to minimize cell activity. Just before adding the solution to the experimental set-up it was diluted 1:20 with Milli-Q water to reduce its conductivity to an appropriate value for forming an EHD bridge.

The experimental set-up was equivalent to that of Ref. [37]. and consisted of two glass beakers filled (66 g) with triply deionized water or the stock solution, respectively, and two platinum electrodes immersed into the liquid. The beakers were placed on a motorized stage where they could be automatically separated. At start-up position the edges of the beakers were in contact and the electrodes were put into the liquids. After applying high DC voltage and the bridge formation, the distance between the beakers was slowly increased to approximately 1 cm. One experimental series consisted of three different configurations:

a) Stock solution in both beakers (66 g solution anolyte and catholyte)
b) Stock solution only in anolyte (66 g solution as anolyte and 66 g Milli-Q water as catholyte)
c) Stock solution only in catholyte (66 g solution as catholyte and 66 g Milli-Q water as anolyte).

Conductivity and temperature were measured in each beaker before and after running the bridge; approximate values of the average voltage and current during the experiment were recorded as well. One run lasted 5 min unless noted otherwise. In order to avoid confusion concerning control and catholyte when abbreviations are used, all control experiments are referred to as “blank”. After the experiment 4.5 mL samples were taken from both beakers and the blank (as blank the 1:20 diluted stock solution was used) and added to the Greiner tubes with 4.5 mL 2x medium. The blank sample constitutes the control experiments to which the other results are compared. One of these tubes was filled with Milli-Q water as blind for the OD measurement. Since one series comprised 3 experiments, one experimental session resulted in 10 different samples (Experiment **a** Anolyte, Experiment **a** Catholyte, Experiment **a** Blank, Experiment **b** Anolyte, Experiment **b** Catholyte, Experiment **b** Blank, Experiment **c** Anolyte, Experiment **c** Catholyte, Experiment **c** Blank, and Blind). From each sample, dilution series in phosphate buffered saline (PBS buffer) were made and plated on agar plate for counting the colony forming units (CFU). The plates were incubated at 25 °C for 24 h. The plates inoculated with algae solution were incubated 1 week at 25 °C under appropriate illumina-

tion. The Total cell number (TCN) of the samples was also measured by counting the cells under a microscope using counting chambers. Directly after the experiment the OD of the samples was measured using a spectrophotometer in a transparent 96 well plate (200 µL sample per well) at 490 nm. The measurements were repeated after 24 and 48 h to study and compare the cell growth rate. The algae cultures were measured after 5–6 days and 8–9 days. Between the measurements the samples were kept at 25 °C in their respective incubator.

Additionally one series of experiments was conducted with a human monocytic cell line (THP-1). These experiments were conducted at the cell culture laboratory at the Institute of Hygiene, Microbiology and Environmental Medicine in Graz, Austria. THP 1 cells were grown in RPMI 1640 medium + 10% FBS + 2 mM L-Glutamine + 25 mM Hepes (Gibco, Germany), at 37 °C. Cells were suspended, counted and harvested by centrifugation (8 min, 400g). After washing with 20 mL glucose solution (5%) cells were resuspended in 11 mL glucose solution (5%) and counted. This stock solution was diluted right before the experiments (2.5 mL suspension + 64 mL milliQ water). Experimental series **a**, **b** and **c** were conducted as described above. Cell counts were measured in a 5 mL sample withdrawn from each beaker using a cell counter (Schärfe CASY-1 TTC, Omni Life Science GmbH & Co. KG, Bremen, Germany) right after the experiments. Temperature of the cell solutions was recorded before and after the experiment.

2.2. Zeta potential measurements

The zeta potential was measured in deionized water and in PBS buffer solution using a Nano ZS Zetasizer (Malvern Instruments Ltd, Worcestershire, UK) by means of electrophoretic light scattering (0.12 µm cm/V s for aqueous systems using NIST SRM1980 standard reference material). The system was calibrated using its integrated auto-calibration.

2.3. Visualization

The transport of algae and yeast through the bridge was visualized by means of an additional run with a high microbial load (McFarland 0.5; $5{\cdot}10^6$ cells mL^{-1}). Microorganisms were added to both beakers. The bridge was observed and recorded with a Panasonic HDC SD-600 HDTV video camera.

2.4. Electric current model

The current in the water bridge was calculated using the electric current module in Comsol 4.4 and 5.2 multiphysics software (Comsol Inc., Palo Alto, CA) using a 3D model described in detail earlier [37] which was placed in a spherical air bubble. For each microorganism average values of measured potentials and conductivities from the experiments were used to calculate the current density in the bridge. For the simulation of the current densities in the bridge average values of the experimental values of conductivity and potential were used. The current density was calculated as average value along a 1 cm line in the center of the simulated bridge since a cross-section of the simulation shows that there is an equal radial distribution of current density in the model. These current densities were applied in the 2D models in order to study the current flow through the cells.

3. Results

3.1. Zeta potential, mobility and electrophoretic migration velocity

The electrophoretic mobility μ_p can be derived from the zeta potential ζ using the Henry equation,

Table 1
Zeta potential, mobility and velocity of organisms and PBMC (peripheral blood mononuclear cells, including monocytes) in EHD bridging solutions and/or buffers. For the calculations of the velocity and the mobility, an electric field of $E = 4{\cdot}10^5$ V/m [37] and a dynamic viscosity of $\eta = 8.9{\cdot}10^{-4}$ Pa s were used. "0" and "0.0" errors mean that the error was lower than the displayed precision.

Organism	ζ/mV	$\mu_p/10^{-8}$ m^2 V^{-1} s^{-1}	V_E/mm s^{-1}
E. coli (milli-Q water)	−39 ± 2	−3.1 ± 0.1	12.2 ± 0.5
E. coli (PBS)	−13 ± 1	−1.0 ± 0.0	4.1 ± 0.2
E. coli Hu 734[a]	−27 ± 9	−2.1 ± 0.7	8.4 ± 2.8
B. subtilis subtilis (milli-Q water)	−39 ± 2	−3.0 ± 0.2	12.1 ± 0.9
B. subtilis subtilis (PBS)	−20 ± 1	−1.6 ± 0.1	6.3 ± 0.2
B. subtilis subtilis (pH 6, vegetative cells, ATCC15561)[b]	−54 ± 3	−4.2 ± 0.2	17 ± 0.9
B. subtilis subtilis (pH 6, vegetative cells, ATCC12695)[b]	−35 ± 3	−2.7 ± 0.2	11 ± 0.9
N. oleoabundans (milli-Q water)	−34 ± 2	−2.7 ± 0.2	10.6 ± 0.6
N. oleoabundans (PBS)	−22 ± 2	−1.7 ± 0.2	6.9 ± 0.7
N. oleoabundans[c]	−17 ± 2	−1.3 ± 0.2	5.3 ± 0.6
S. cerevisiae (milli-Q water)	−24 ± 1	−1.9 ± 0.1	7.4 ± 0.2
S. cerevisiae (PBS)	−6 ± 1	−0.5 ± 0.1	1.8 ± 0.2
S. cerevisiae (stationary phase)[d]	−11 ± 1	−0.9 ± 0.1	3.4 ± 0.3
S. cerevisiae (exponential phase)[d]	−18 ± 2	−1.4 ± 0.2	5.6 ± 0.6
S. cerevisiae (death phase)[d]	−17 ± 1	−1.3 ± 0.1	5.3 ± 0.3
PBMC (buffer)[e]	−12 ± 1	−0.9 ± 0.1	3.7 ± 0.2
PBMC (PBS)[f]	−22 ± 0	−1.7 ± 0.0	6.8 ± 0.1

[a] Value from [40].
[b] Value from [41].
[c] Value from [42].
[d] Value from [43].
[e] Value from [44].
[f] Value from [45].

$$\mu_p = \frac{2\varepsilon\zeta f(K_a)}{3\eta}, \tag{1}$$

where ε the dielectric constant, η the viscosity and $f(K_a)$ Henry's function. In aqueous media, $f(K_a)$ is 1.5, which is also referred to as Smoluchowski's approximation. Zeta potentials ζ are compared to literature values in Table 1 which also provides electrophoretic mobilities μ_p, and electrophoretic migration velocities V_E. Values of organisms with superscript letters were taken from the literature as indicated, the others were measured as described in Section 2.2 and calculated from the Stoke's equation as described previously [37] and in Eq. (1), respectively. All values displayed were rounded according to their measurement precision; for the calculations in between the columns full precision was used.

3.2. Visualization

Fig. 1 shows the time dependent transport of the algal (a–e) and yeast cells (f–j) in an EHD bridging set-up. The time between each image is 2 min 30 s. In both cases the transport from the catholyte to anolyte can be clearly seen by the formation of a clear area at the top part of the catholyte growing downwards with time. Simultaneously the optical density of the microbial solution in the anolyte increases as can be seen by the intensifying turbidity. Algae are apparently transported faster and yeast cells are transported slower than *E. coli.* if one compares the present data to an earlier study [37]. An estimation based on the turbidity decrease of the upper half of the catholyte shows that approximately after 2.5 min (or even less), 50% of the algae; and after ~7.5 min 50% of the yeast cells are transferred to the anolyte. This result is in agreement with the higher electrophoretic velocity of the algae in milliQ water (see Table 1). With a starting concentration of $5{\cdot}10^6$ cells mL^{-1}, each beaker initially contains $3.3{\cdot}10^8$ microorganisms, yielding a transport rate of $1.1{\cdot}10^6$ algal and $3.7{\cdot}10^5$ yeast cells per second, respectively. With a volume of ~65 µm^3 for both algal [46] and

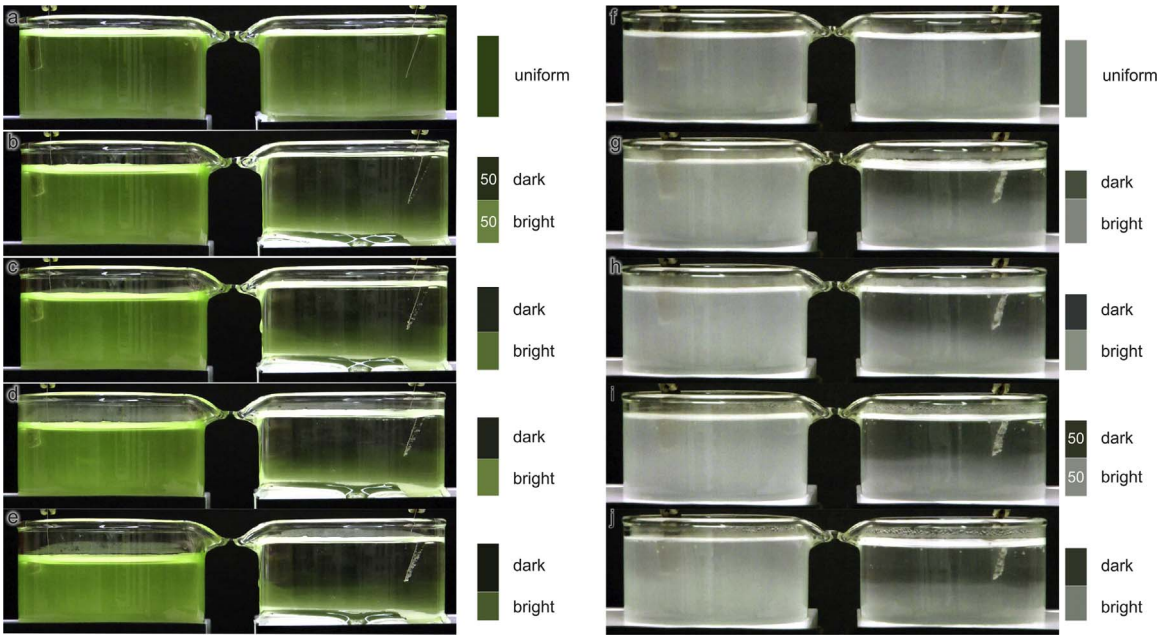

Fig. 1. Horizontal aqueous liquid bridge with algae (a–e) and yeast (f–j) in both beakers ($5{\cdot}10^6$ cells mL^{-1}; anolyte left, catholyte right). Pictures were taken at 2.5 min intervals starting at 0 min. Note the region with lower microbial density growing downward in the catholyte with increasing microbial density (turbidity) in the anolyte.

yeast cells [47], and an electrophoretic velocity of $10.6{\cdot}10^{-3}$ ms^{-1} ($7.4{\cdot}10^{-3}$ ms^{-1}) an effective bridge diameter for these experiments is 0.09 mm or ~5% (0.06 mm or ~3%) of the total diameter for algal and yeast cells, respectively. As is the case for the bacteria only a small part of the bridge transports the microorganisms; and this part is the outer layer of the bridge due to its rotation and the electrostatic repulsion of the microorganisms [15,37].

3.3. Fluid velocity

The forces within a floating EHD bridge have been described in detail previously [6,9,15,37]. They show that the forces due to the Maxwell stress tensor [6,9] result in transport velocities approximately 20 times higher [37] than the electrophoretic velocities given in Table 1, thereby explaining why all microorganisms are always transported in both directions. The electrical force mitigates the transport against their electrically preferred direction, and facilitates the opposite.

3.4. Experiments with Bacillus subtilis subtilis

Table 2 presents the approximate minimum and maximum values of voltage and current for 3 series of 3 experiments (3 repetitions) as well as conductivity and temperature before and after bridge operation. All experiments lasted 5 min.

After the bacterial experiments, CFU, TCN and OD measurements were performed in order to investigate the viability of the organisms after exposure (see Fig. 2). During most experiments a manual voltage increase during the operation was necessary because the bridge became thinner and unstable over time due to a conductivity increase. The usual voltage was 10–13 kV with the exceptions of experiment 1**a** and experiment 2**c**, where higher voltages (18.1 and 20.3 kV) were required. The current fluctuated between 0.3 and 0.8 mA, except in experiment 1**a**, because in this experiment the starting conductivity of the bacterial solution was higher than usual. The conductivity of the anodic solution showed always a significant increase after the experiment; in the catholyte both increase and decrease of conductivity were observed. In experiment 1**a** and experiment 2**c** blue discharges were observed during bridge operation causing cell destruction which allowed salts from the cell plasma to diffuse into the solution, thereby additionally increasing the conductivity (see Table 3). The temperature increased in both beakers in all experiments by values between 1.7 and 8.3 °C, respectively. As representative example for all three series the CFU results from series 1 are shown in Fig. 2a. Like *E. coli, B. subtilis*

Table 2
Time, voltage, current, conductivities and temperatures of the experiments with *B. subtilis subtilis*. **S**…Series, **E**… Experiment, Experiment **a**: stock solution in both beakers, experiment **b**: stock solution in anolyte, experiment **c**: stock solution in catholyte.

S	E	U/kV	I/mA	σ/μS/cm				Θ/°C			
				Anolyte		Catholyte		Anolyte		Catholyte	
				Before	After	Before	After	Before	After	Before	After
1	**a**	12.5–18.1	1.0–2.0	2.20	6.27	2.21	1.86	16.4	20.7	16.8	25.1
	b	12.0	0.4	1.52	2.13	0.95	0.89	11.3	16.1	12.2	16.5
	c	12.0–13.2	0.5	1.14	1.67	1.59	1.40	14.1	18.9	14.2	18.9
2	**a**	10.5–12.3	0.4–0.6	1.46	1.97	1.50	1.77	7.7	15.2	8.1	13.8
	b	11.0	0.4–0.5	1.35	1.95	0.86	1.13	10.9	16.2	12.4	15.9
	c	11.2–12.5	0.4	1.01	1.49	1.36	1.43	14.1	18.1	9.1	13.7
3	**a**	10.6–12.0	0.3	1.64	2.33	1.81	2.13	16.4	18.1	11.6	13.6
	b	12.1–20.3	0.6–0.8	1.84	4.75	0.88	1.43	10.9	18.4	13.2	18.5
	c	12.0	0.6	0.83	1.78	1.86	1.88	16.4	19.5	11.6	16.5

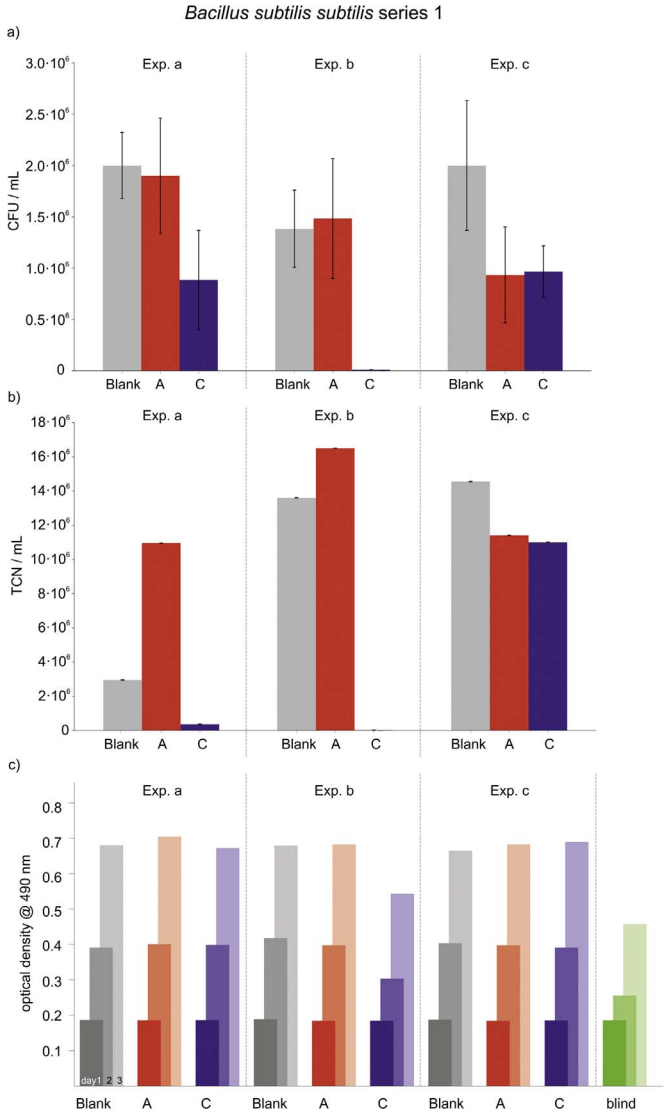

Fig. 2. (a) CFU, (b) TCN per mL of the experiments with *B. subtilis subtilis*, and (c) OD results after 0, 24 and 48 h from series 1 of the experiments with *B. subtilis subtilis*; series 1. experiment **a**: stock solution in both beakers, experiment **b**: stock solution in anolyte, experiment **c**: stock solution in catholyte.

subtilis carry a negative surface charge and are thus mainly drawn to the anode [37]. There was no significant difference in experiments **a** and **c**; in experiment **b** the blank showed the highest count, followed by the anolyte (where the bacteria were added). No (alive) bacteria were transported to the catholyte in this experiment. When looking at the TCN results, it seems that rather than being killed by the transport, no bacteria were present in catholyte at all; whereas in experiment **a**, when initially present in both beakers, cells were transported from the catholyte into the anlyte. The total cell number for series one is given in Fig. 2b. Like *E. coli* [37] most of the cells seemed to survive the process. This assumption is also supported by the fact that conductivity, normally associated with ion release caused by cell death, increased only slightly during the process unless discharges occurred. The OD measurements done directly afterwards, 1 day and 2 days after the experiment show comparable growth rates of all bacteria (see Fig. 2c). Those not exposed (blank), those exposed to the set-up, and those who certainly did undergo transport through the bridge (C in experiment **b**, and A in experiment **c**). The only outlier is the value of the bacteria which were transported from anolyte to catholyte after 2 days (experiment **b** / C).

3.5. Experiments with Neochloris oleoabundans

Voltage, current, conductivity and temperatures of 3 series of 3 experiments (3 repetitions) with *Neochloris oleoabundans* are given in Table 3. All experiments lasted 5 min except 3**a** (5 min 45 s) and 3**c** (5 min 10 s).

The voltage showed the same behavior as during the experiments with bacteria; the current values were generally a bit higher than those measured during the bacterial experiments, though. Blue discharge was observed at series 1 experiment **b** and series 2 experiment **b**. The conductivity increased in all experiments in the anolyte and some of the experiments in the catholyte as well. The temperature was always higher in both beakers after running the bridge, just like during the bacteria experiments. The smallest temperature difference was 2.5 °C, the biggest 8.4 °C. After the algae experiments, TCN and OD measurements were performed in order to investigate the viability of the organisms after exposure (see Fig. 3). CFU measurements were tried but turned out unsuccessful, as algae do not favor growth on plates. The reproducibility of the algae TCN experiments was high enough to combine all three series into one statistic which is given in Fig. 3a. Like the other organisms investigated before, the algae carry a negative surface charge, and were therefore drawn to the anode. Concerning cell transport the algae experiments followed the same trend as *B. subtilis subtilis*. In experiment **a** more cells were counted in the anolyte, in experiment **b** almost no cells were observed in the catholyte, and in experiment **c** a significant number of cells was transported to the anolyte (Fig. 3a). The OD measurements for this organisms (Fig. 3b) were done directly after the experiment (day 1) as well as 6 and 9 days later due to the slower growth rate of these algae. As representative example, the results of series 3 are given in Fig. 3b. In all experiments, the algae exposed to the set-up showed a decreased growth compared to

Table 3
Time, voltage, current, conductivities and temperatures of the experiments with *N. oleoabundans*. **S**…Series, **E**… Experiment, Experiment **a**: stock solution in both beakers, experiment **b**: stock solution in anolyte, experiment **c**: stock solution in catholyte.

S	E	U/kV	I/mA	σ/μS/cm				ϴ/°C			
				Anolyte		Catholyte		Anolyte		Catholyte	
				Before	After	Before	After	Before	After	Before	After
1	**a**	11.5	0.7	1.95	3.91	1.97	2.19	7.2	15.6	8.7	15.7
	b	13.0	0.7	2.05	4.38	0.96	1.62	9.3	17.1	9.8	18.2
	c	13.1–16.6	1.5	0.83	2.48	1.91	1.72	12.6	21.0	10.3	18.3
2	**a**	10.2	0.5	2.10	3.89	2.05	1.94	8.2	14.3	9.3	14.3
	b	10.2	0.4	1.95	3.33	1.17	1.37	12.2	16.9	10.3	16.4
	c	10.2	0.5–1.0	1.18	2.62	1.96	1.75	13.7	18.7	8.7	15.6
3	**a**	10.0	1.3	1.75	3.56	1.82	1.95	7.4	13.9	9.2	13.9
	b	11.4–12.2	0.4	1.72	2.17	0.87	1.27	10.5	14.8	11.2	15.1
	c	10.0	0.3	0.99	1.48	1.64	1.67	14.3	16.8	8.6	12.7

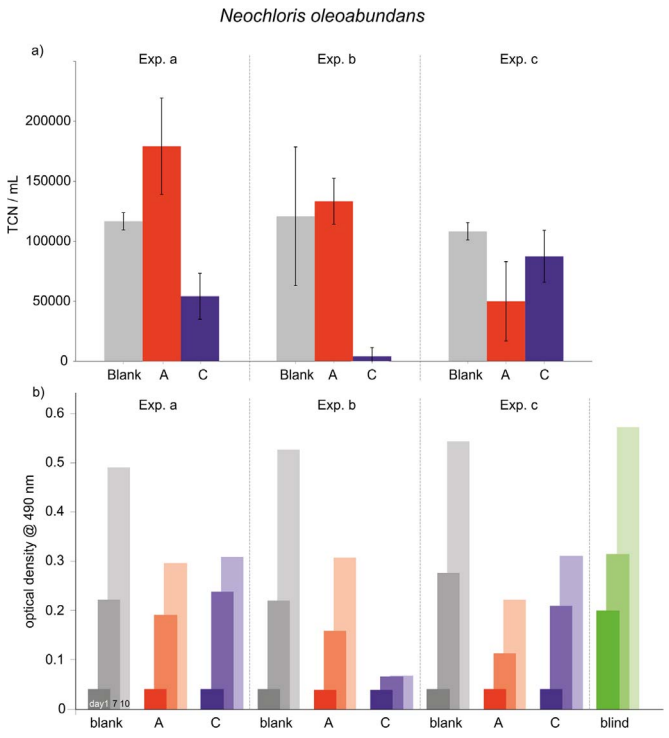

Fig. 3. (a) TCN results in cells/mL from series 1, 2 and 3 and (b) OD results after 0, 6 and 9 days from series 3 of the experiments with *N. oleoabundans;* experiment **a**: stock solution in both beakers, experiment **b**: stock solution in anolyte, experiment **c**: stock solution in catholyte.

the blank; and those transported through the bridge (C in experiment **b** and A in experiment **c**) showed an even lower growth rate.

3.6. Experiments with Saccharomyces cerevisiae

Voltage, current, conductivity and temperatures of 3 series of 3 experiments (3 repetitions) with *Saccharomyces cerevisiae* are given in Table 4. All experiments lasted 5 min.

Conductivity and temperature behaved comparably to the experiments with *B. subtilis subtilis* and *N. oleoabundans*. The conductivity was always higher in the anolyte while in the catholyte both slightly higher and lower values were measured after bridge operation. Blue discharges were only observed during series 1 experiment **a** where the conductivity increased slightly. The temperatures measured at the end were always higher than the beginning. The smallest difference was 1.1 °C, the biggest 8.8 °C. CFU, TCN and OD measurements were performed in order to investigate the viability of the organisms after exposure (see

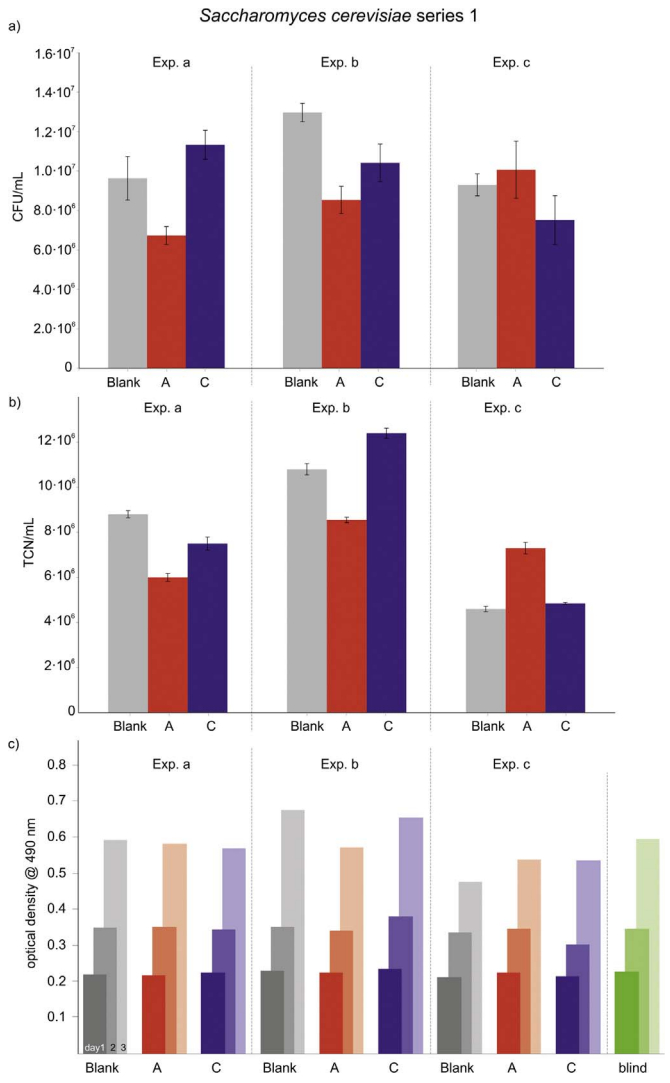

Fig. 4. (a) CFU/mL results from series 3, (b) TCN results in cells/mL from series 1 and (c) OD results after 0, 24 and 48 h from series 1 the experiments with *S. cerevisiae;* experiment **a**: stock solution in both beakers, experiment **b**: stock solution in anolyte, experiment **c**: stock solution in catholyte; A…anolyte, C…catholyte.

Fig. 4). The CFU results of series 1 are shown in Fig. 4a as representative example. They are different from the values obtained from all other organisms so far. At low concentrations the yeast cells do not show a preferred flow direction probably due to their low surface charge.

The results of OD measurements at 490 nm are shown in Fig. 4c,

Table 4
Time, voltage, current, conductivities and temperatures of the experiments with *S. cerevisiae.* **S**…Series, **E**… Experiment, Experiment **a**: stock solution in both beakers, experiment **b**: stock solution in anolyte, experiment **c**: stock solution in catholyte.

S	E	U/kV	I/mA	σ/μS/cm				Θ/°C			
				Anolyte		Catholyte		Anolyte		Catholyte	
				Before	After	Before	After	Before	After	Before	After
1	**a**	9.7	0.3	1.72	2.43	1.65	1.58	7.6	13.4	6.6	11.9
	b	9.1	0.3	1.63	2.40	1.19	1.14	7.5	14.0	10.3	15.1
	c	9.7	0.6	1.12	2.01	1.63	1.43	12.4	17.1	7.8	13.7
2	**a**	9.5	0.7	1.89	3.16	1.96	1.83	7.7	13.9	6.8	12.3
	b	9.5	0.3–0.5	1.63	2.53	1.16	1.21	8.9	14.2	10.0	15.0
	c	9.5	0.4	1.21	1.56	1.74	2.31	12.2	13.3	8.0	16.8
3	**a**	10.4	1.0	3.10	6.02	2.70	2.63	9.7	15.3	8.9	15.5
	b	9.5	0.7	2.73	4.62	2.13	2.08	17.4	19.7	17.4	20.0
	c	9.5–10.4	0.5–0.8	2.11	3.86	2.61	2.30	17.5	19.7	11.8	16.7

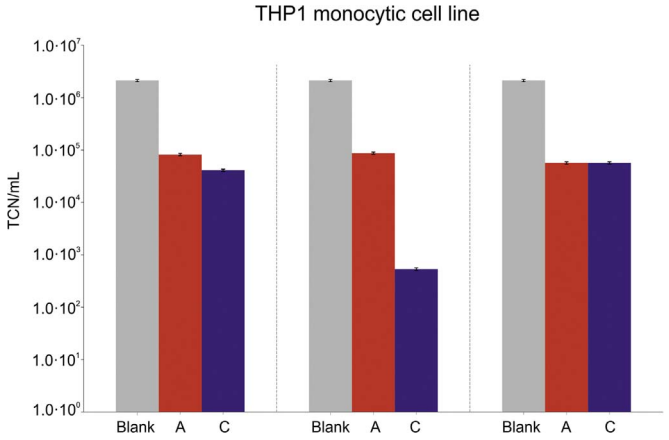

Fig. 5. TCN results in cells/mL of the experiments with THP-1; experiment **a**: stock solution in both beakers, experiment **b**: stock solution in anolyte, experiment **c**: stock solution in catholyte; A…anolyte, C…catholyte.

again series 1 was chosen as representative example. Unlike the results of *N. oleoabundans* OD measurements do not indicate a negative effect on growth rate of the organism.

3.7. Experiments with the THP-1 human cell line

In order to properly display these results a logarithmic scale was chosen (see Fig. 5) since most of these cells were killed in the experiment. Due to their negative surface charge the transportation behavior is similar to the one observed from the bacterial and algal cells.

3.8. Simulation of the current density

Fig. 6 shows the simulation results of the bridge (a) and the organisms exposed to the average current density in the bridge (b–f). Physical parameters for the calculations are given in Table 5. The potentials and conductivities of the surrounding water are averaged from the experimental data (Tables 2–4 ,[43] for *E. coli*.). For the monocytes the same values as for *E. coli* were assumed. The potentials used on the simulation boxes were calculated so that an empty box would reveal the same current density as in the bridge. These empty boxes are thus 2D representatives of electrical conditions in the bridge. In the center of each box a respective organism simulation was added; the current redistribution due to the presence of the organism was calculated and the results are visualized in Fig. 6.

The ranges of the color scales were chosen manually in order to visualize the current flow most effectively whilst maintaining comparability. In case (a) only values above 0.0001 mA cm^{-2} are displayed so that glass beakers and surrounding air are not colored. A "+" sign and the arrow in the color scale mean that values higher than the maximum scale value (7 mA cm^{-2} for a, 100 mA cm^{-2} for b-e and 50 mA cm^{-2} for f) are shown in the same color (dark red). In case of *E. coli* and *B. subtilis subtilis* (Fig. 6b and c) the current is channeled through the cell wall, no current enters the cell body. *S. cerevisiae* (Fig. 6e) shows a similar response, the current is mostly channeled through the outer part of the cell wall, no current enters the cell. *N. oleoabundans* is only weakly protected by its cell wall, allowing a part of the current flowing though the cell, additionally the liposomes are acting as current lenses, forming high current density regions in the cell plasma (Fig. 6d). The human monocyte (THP-1) is drastically affected by the current in the bridge, the cell membrane offers no protection for the cell (Fig. 6f).

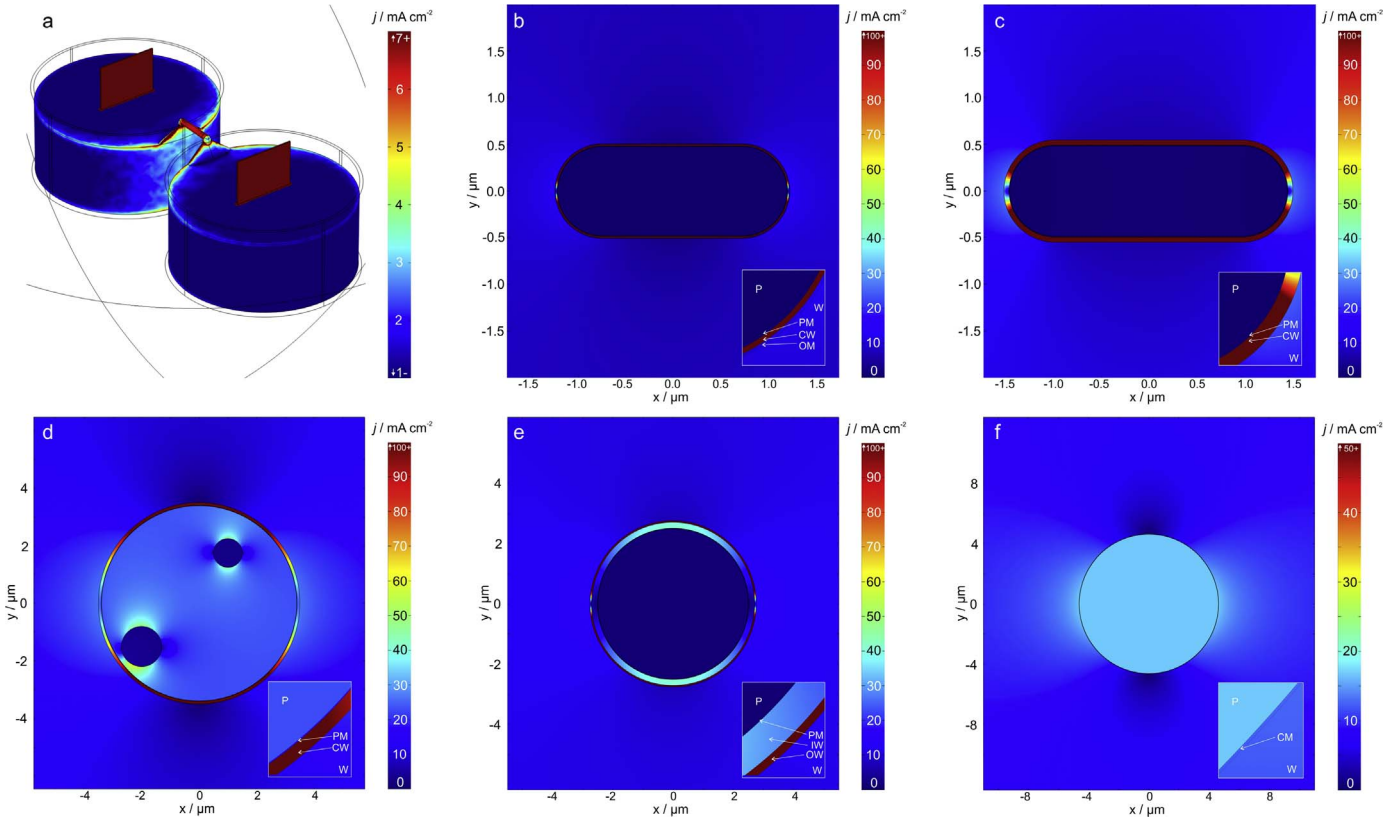

Fig. 6. Simulation results. a: 3D water bridge model for pure water, b–f: microorganisms exposed to the current density in the field (see Table 1 for simulation parameters; W: water, P: plasma, OM: outer membrane; CW: cell wall; IW: inner cell wall, OW: outer cell wall, PM: plasma membrane): b: *E. coli*, c: *B. subtilis subtilis,* d: *N. oleoabundands*, e: *S. cerevisiae*, f: THP-1. The inserts show magnifications of the layer structure of the cell boundaries; the two dark circles inside the alga (d) are simulated liposomes.

Table 5
Physical parameters for the simulations of the organisms in the electric field (Fig. 6). For Fig. 6a (3D bridge model), the conductivity of pure distilled water (0.8 μS cm^{-1}) was used. U_{wb} is the average potential applied to the experiment, U_{box} is the potential applied to the simulation box in order to simulate the current density *j*. n.a. = not applicable, *E. coli* values from [48,49], *S. cerevisiae* values from [50], *B. subtilis subtilis* thickness values from [51] and values for permittivity and conductivity are approximated by values for *S. aureus* and *S. epidermidis* from [48,52], respectively. Cytoplasm values for THP-1 monocytes are derived from [53], membrane values from [54]. Values for *N. oleoabundans* from [55].

	Outer membrane			Wall inner (outer)			Plasma membrane			Cytoplasm	
	ε	σ/S m^{-1}	*d*/μm	ε	σ/S m^{-1}	*d*/μm	ε	σ/S m^{-1}	*d*/μm	ε	σ/S m^{-1}
E. coli	10	$2{\cdot}10^{-6}$	0.008	60	0.5	0.015	10	$5{\cdot}10^{-8}$	0.008	60	0.1
B. subtilis subtilis	n.a.	n.a.	n.a.	60	0.01	22.3 (33.3)	4.5	$5{\cdot}10^{-8}$	6.6	70	0.8
S. cerevisiae	n.a.	n.a.	n.a.	60 (6.2)	0.0012 (0.021)	0.2 (0.005)	5	$1{\cdot}10^{-7}$	0.008	53	1
N. oleoabundans	n.a.	n.a.	n.a.	75	0.05	0.1	8	$2{\cdot}10^{-5}$	0.008	50	0.5
THP-1 monocytes	n.a.	n.a.	n.a.	n.a.	n.a.	n.a.	80	0.01	0.005	126.8	0.56
	U_{wb}/kV			Box size/μm^2		σ_{water}/S m^{-1}		*j* /mA cm^{-2}		U_{box}/V	
E. coli	12.74			10·10		$1.174{\cdot}10^{-4}$		8.01		6.82	
B. subtilis subtilis	12.63			10·10		$1.785{\cdot}10^{-4}$		12.07		6.76	
S. cerevisiae	9.65			20·20		$2.190{\cdot}10^{-4}$		11.34		10.33	
N. oleoabundans	11.31			20·20		$2.005{\cdot}10^{-4}$		12.14		12.11	
THP-1 monocytes	12.74			40·40		$1.174{\cdot}10^{-4}$		8.01		27.30	

4. Discussion

4.1. Cell transport

The charge of the cell wall is different from species to species, so it is not surprising that the electrophoretic behavior of the algae and the yeast differs from that of the bacteria. Table 1 provides an overview over zeta potentials and electrophoretic mobilities of the cells used [56]. The potential is generally higher in pure water than in buffer solution. This is due to the lower amount of charges (ions) present in pure water, which allow the cells to move more freely and without the attraction (and thus impediment) of counter ions. Whereas the potentials of all cells are in the same order of magnitude, an alga, like any eukaryotic cells, measures 10–100 μm, thus ten times the size of a prokaryotic cell. Therefore more electrical energy is required to move them, and it can be expected that their transport rate is lower than that of the bacteria. This is indeed the case, as can be seen by comparison of Figs. 2b and 3a; especially experiment **a**. Apart from that, due to their negative surface charge, the electrically preferred transport direction is, in both cases, from cathode (-) to anode (+) beaker. The transport observed against this direction can be explained by the "back flow mechanism" due to hydrostatic and dielectric forces (see also [37]). *S. cerevisiae* showed a different transport behavior than the bacteria and algae for the lower concentration experiments. Cell transport was observed in both directions with almost the same rate. The absence of a preferred flow direction means that electric forces play a smaller role here than for the other organisms. This conclusion is corroborated by the zeta potential, which is indeed lowest for the yeast cells (see Table 1). Yeast cells are merely dragged along with the liquid, which, when averaged over time, evenly flows in both directions. Because of the low surface charge of yeast, the transport rate was lowest compared to the other organisms.

4.2. Cell behavior

4.2.1. Cytolysis

A cell can burst when excess water is allowed to move into its interior. This situation occurs in a hypotonic environment like in the present case when the cells are added to the deionized water before the experiments. In order to prevent it, cells open their water channels to allow water to come in, and their ion channels to allow ions to exit. This process counteracts the osmotic pressure and can prevent cytolysis unless cell volume increases to the point the cell membrane ruptures due to excessive water influx. The presence of a cell wall protects the membrane and can prolong cell life, sometimes even prevent cytolysis. In the present experiments, all cells experience a hypotonic environment before the bridge is started, and it explains why it is important to start the bridges directly after inoculation; otherwise all organisms might be dead before the voltage is applied. Once the bridge is running, the situation changes as described in the next paragraph.

4.2.2. Organisms in the protonic maelstrom

We have shown that *E. coli* exhibit enhanced growth and activity after being transported through the bridge [37]. The behavior of *B. subtilis subtilis* is more dependent on the location than on the transport: They revealed a higher TCN in the anolyte (Fig. 2b) than in the blank, but a lower OD in the catholyte after two days (Fig. 2c). In all experiments the CFU count was higher than in the catholyte (Fig. 2a), allowing the conclusion that these organisms prefer an oxidative (anodic) environment over a reductive (cathodic) one [21]. Most importantly, however, is that both bacteria survive the exposure quite well, where the gram-negative *E. coli* apparently do better than the gram-positive *B. subtilis subtilis*. The simple 2D model calculations for both bacteria (Fig. 6b and c) show similar results and can tell us why the bacteria survive: The electrical conductivity of a cell wall is higher than that of a cell membrane (see Table 5), so most of the current (in this case made of protons) is directed through the cell wall and does not penetrate the cell, thereby protecting the cell both osmotically and electrically. Ions leaking from the cell wall into the surrounding water are replaced by protons, the current runs mostly through the cell wall, and so the osmotic pressure is maintained although the environment is hypotonic. This effect is a bit stronger for the threefold-protected *E. coli*. than for the *B. subtilis subtilis* with only two boundary layers as can be seen from the slightly brighter areas left and right of the bacteria. This effect (higher charge accumulation at the entrance and exit points of the cell) accompanies current running through the inside of the cell. *N. oleoabundans* (Fig. 6d) is an example thereof, and the growth experiments indeed show an adverse effect on the organism: Although protected against cytolysis by a thick cell wall; algae which underwent transfer through the bridge (and therefore exposure to the highest current densities) exhibit a much slower growth rate than those in the beaker of origin and the blank (Fig. 3b). The simulation (Fig. 6d) clearly shows that algae are not as well protected as the bacteria and current passes through the cell interior, too. Moreover, liposomes which can be present inside these algae act as electrical isolators and create zones of higher current densities within the cells, thereby enhancing the osmotic pressure and proton concentration inside the cell. So in contrast to the bacteria, algae largely suffer from the exposure to the proton current. The cells more likely to survive are those with the smallest amount of liposomes, which explains their strongly weakened growth (see Fig. 3b). The opposite is true for the yeast: They are similarly sized as the algae, but very well protected by an array of cell wall and

membranes which effectively divert the proton current from entering the cells. This is a clear indication that the importance electrical behavior of the cells' exterior supersedes that of their size when it comes to survival in this environment. The situation of yeast cells is, concerning their electrical properties, comparable to the situation of *E. coli*, and so is their behavior after exposure: The CFU count is higher for those cells which went through the bridge when compared to the blank (see Fig. 4a), and most of the cells survive. Finally, the monocytic human THP-1 cells are the least protected. In lack of a Faraday cage (a conducting cell wall) they reveal the highest internal current densities (see Fig. 6f). Only very few (5–10%) survive the experiment (note the logarithmic scale in Fig. 5 in contrast to the linear scales in Figs. 2–4). Given the fact that the experiments last 5 min and that in this case the exposure to the protonic current is not beneficial but adverse to the viability, the fact that *any* THP-1 cells survive at all is quite astonishing. The authors plan to do further research on that in a future study.

5. Conclusions

The behavior of microorganisms in an EHD bridge experiment depends on their electrical properties, their size, their composition and their surface charge. Their transport in depends on obvious parameters: The heavier the organism, the slower the transport; the higher the surface charge, the more pronounced the preferred flow direction. Their viability is dependent on the electrical properties of the respective organism: The right combination of insulating cell membrane and conducting cell wall work as a natural Faraday cage protecting the cells from both the hypotonic environment and the protonic current. This effect was predicted by a simple 2D model (Fig. 6b–f) and was shown experimentally for *E. coli* in a previous work [37] and for *S. cerevisia* and *B. subtilis subtilis* in this work. A low cell wall conductivity (*N. oleoabundands)* or its absence (THP-1 monocytic human cells) allows protons to enter the cell which increases the osmotic pressure and has an adverse effect on their internal biochemical processes, thereby weakening and killing the cells. An EHD aqueous bridge thus provides the possibility to distinguish between different microorganisms based on their electrical properties, a possible application being selective disinfection.

6. Outlook

Apparently electricity can have multiple effects on microorganisms. Dependent on its parameters, it can be lethal (pulsed field with electronic discharges), negligible (weak fields in cell sorting) and beneficial and stimulating (protonic currents for *E. coli* [37]). Strong DC fields and protonic currents inside of water became only recently available via the re-discovery of the “floating water bridge” [1,5], a gel-like state of water [57] with hydrogen bond strengths between those of ice and liquid water [20]. This state of water is probably also present in living cells and across their membranes, where similar electrical conditions are encountered on a much smaller scale [39]. We have shown a hypothesis explaining why some organisms can survive the process more easily than others, allowing selective disinfection depending on the electrical properties of the different cells. Nevertheless this hypothesis calls for additional investigations in view of the fact that protonic conductivity is aqueous media is very different from conductivity based on other regular cations and anions, especially under the influence of strong electric fields [22]. The authors of the present work are planning to conduct additional studies on this matter.

Whereas it is still unclear how the exposure can have a *stimulating* effect as was shown by bioluminescence of genetically altered *E. coli* [37] it is tempting to speculate that the electrical similarity of the water bridge to cell water (strong field and protonic currents) is – in some still unknown way – reason for its stimulating effect on microorganisms. If so, many possible applications come to mind, like, for example, efficiency increase of bioreactors *a priori* or in situ bacterial stimulation. Even medical applications seem feasible. The fact that a few percent of the human cells survived the process line paves the ground for further experiments in that direction which may include (but are not limited to) established processes like electroporation and stimulation of human cells. The authors of this work plan to further investigate these ideas in a subsequent work.

Acknowledgements

This work was performed at Wetsus, European Centre of Excellence for Sustainable Water Technology (www.wetsus.eu) and The Medical University of Graz, Austria. Wetsus is co-funded by the Dutch Ministry of Economic Affairs and Ministry of Infrastructure and Environment, the Province of Fryslân, and the Northern Netherlands Provinces. The authors would like to thank Prof. Jakob Woisetschläger (TU Graz, Austria) and the other participants of the research theme “Applied Water Physics” for the fruitful discussions and their financial support.

Appendix A. Transperancy document

Transparency document associated with this article can be found in the online version at http://dx.doi.org/10.1016/j.bbrep.2017.04.015.

References

[1] W.G. Armstrong, The Newcastle Literary and Philosophical Society, The Electrical Engineer, 1893, pp. 154–155.
[2] F. Mugele, J.C. Baret, J. Phys. Condens. Matter 17 (2005) R705.
[3] I. Sumoto, Oyo Butsuri 25 (1956) 264.
[4] W. Uhlig, personal communication, Laboratory of Inorganic Chemistry, ETH Hönggerberg–HCI, Zürich, 2005.
[5] E.C. Fuchs, J. Woisetschläger, K. Gatterer, E. Maier, R. Pecnik, G. Holler, H. Eisenkölbl, J. Phys. D: Appl. Phys. 40 (2007) 6112–6114.
[6] A. Widom, J. Swain, J. Silverberg, S. Sivasubramanian, Y.N. Srivastava, Phys. Rev. E 80 (2009) 016301.
[7] A.G. Marin, D. Lohse, Phys. Fluids 22 (2010) 122104.
[8] A.A. Aerov, Phys. Rev. E 84 (2011) 036314.
[9] J. Woisetschläger, A.D. Wexler, G. Holler, M. Eisenhut, K. Gatterer, E.C. Fuchs, Exp. Fluids 52 (2012) 193–205.
[10] E.C. Fuchs, MDPI Water 2 (2010) 381–410.
[11] E.C. Fuchs, A.D. Wexler, L.L.F. Agostinho, M. Ramek, J. Woisetschläger, J. Phys: Conf. Ser. 329 (2011) 012003.
[12] R.C. Ponterio, M. Pochylski, F. Aliotta, C. Vasi, M.E. Fontanella, F. Saija, J. Phys. D: Appl. Phys. 43 (2010) 175405.
[13] E.C. Fuchs, B. Bitschnau, J. Woisetschläger, E. Maier, B. Beuneu, J. Teixeira, J. Phys. D: Appl. Phys. 42 (2009) 065502.
[14] E.C. Fuchs, B. Bitschnau, S. Di Fonzo, A. Gessini, J. Woisetschläger, F. Bencivenga, J. Phys. Sci. Appl. 1 (2011) 135–147.
[15] J. Woisetschläger, K. Gatterer, E.C. Fuchs, Exp. Fluids 48 (2010) 121–131.
[16] D. Rai, A.D. Kulkani, S.P. Gejiji, R.K.J. Pathak, J. Chem. Phys. 128 (2008) 034310.
[17] Y.C. Choi, C. Pak, K.S. Kim, J. Chem. Phys. 124 (2006) 094308.
[18] A.M. Saitta, F. Saija, P.V. Giaquinta, Phys. Rev. Lett. 108 (2012) 207801.
[19] E.M. Stuve, Chem. Phys. Lett. 519–520 (2012) 1–18.
[20] L. Piatkowski, A.D. Wexler, E.C. Fuchs, H. Schoenmaker, H.J. Bakker, PCCP 14 (2012) 6160–6164.
[21] M. Sammer, A.D. Wexler, P. Kuntke, H. Wiltsche, N. Stanulewicz, E. Lankmayr, J. Woisetschläger, E.C. Fuchs, J. Phys. D: Appl. Phys. 48 (2015) 415501.
[22] E.C. Fuchs, B. Bitschnau, A.D. Wexler, J. Woisetschläger, F.T. Freund, J. Phys. Chem. B 119 (52) (2015) 15892–15900.
[23] E.C. Fuchs, A. Cherukupally, A.H. Paulitsch-Fuchs, L.L.F. Agostinho, A.D. Wexler, J. Woisetschläger, F.T. Freund, J. Phys. D: Appl. Phys. 45 (2012) 475401.
[24] A.D. Wexler, M. López Sáenz, O. Schreer, J. Woisetschläger, E.C. Fuchs, J. Vis. Exp. 91 (2014) e51819.
[25] H. Andersson, A. Van den Berg, Sens. Actuators B: Chem. 92 (2003) 315–325.
[26] C. Yi, C.W. Li, S. Ji, M. Yang, Anal. Chim. Acta 560 (2006) 1–23.
[27] H. Tsutsui, C.M. Ho, Mech. Res. Commun. 36 (2009) 92–103.
[28] D.R. Gossett, W.M. Weaver, A.J. Mach, C. Hur, H.T. Kwong, W. Lee, H. Amini, D. Di Carlo, Anal. Bioanal. Chem. 397 (2010) 3249–3267.
[29] N.M. Calvin, P.C. Hanawalt, J. Bacteriol. 170 (1988) 2796–2801.
[30] C. Chen, S.W. Smye, M.P. Robinson, J.A. Evans, Med. Biol. Eng. Comput. 44 (2006) 5–14.
[31] M.B. Fox, D.C. Esveld, A. Valero, R. Luttge, H.C. Mastwijk, P.V. Bartels, A. van den Berg, R.M. Boom, Anal. Bioanal. Chem. 385 (2006) 474–485.
[32] W.K. Neu, J.C. Neu, Card. Bioelectr. Ther. 2 (2009) 133–161.
[33] P.T. Johnstone, P.S. Bodger, IPENZ Trans. 24 (1997) 30–35.
[34] J. Mosqueda-Melgar, P. Elez-Martínez, R.M. Raybaudi-Massilia, O. Martín-Belloso, Crit. Rev. Food Sci. Nutr. 48 (2008) 747–759.
[35] C. Gusbeth, W. Frey, H. Volkmann, T. Schwartz, H. Bluhm, Chemosphere 75 (2009)

228–233.
[36] C.Y. Hwang, S. Jung, Y.S. Hwang, B.C. Cho, Water Air Soil Pollut. 213 (2010) 161–169.
[37] A.H. Paulitsch-Fuchs, E.C. Fuchs, A.D. Wexler, F.T. Freund, L.J. Rothschild, A. Cherukupally, G.J.W. Euverink, Phys. Biol. 9 (11) (2012) 026006.
[38] A.D. Wexler, S. Drusová, J. Woisetschläger, E.C. Fuchs, PCCP 18 (2016) 16281–16292.
[39] K.M. Tyner, R. Kopelman, M.A. Philbert, Biophys. J. 93 (4) (2007) 1163–1174.
[40] H.C. van der Mei, H.J. Busscher, Appl. Environ. Microbiol. 67 (2001) 491–494.
[41] F. Ahimou, M. Paquot, P. Jacques, P. Thonart, P.G. Rouxhet, J. Microbiol. Methods 45 (2001) 119–126.
[42] E.S. Beach, M.J. Eckelman, Z. Cui, L. Brentner, J.B. Zimmerman, Bioresour. Technol. 121 (2012) 445–449.
[43] W.R. Bowen, R.W. Lovitt, C.J. Wright, J. Colloid Interface Sci. 237 (2001) 54–61.
[44] M.M. Ribeiro, M.M. Domingues, J.M. Freire, N.C. Santos, M.A. Castanho, Front. Cell Neurosci. 6 (2012) 44.
[45] O.V. Bondar, D.V. Saifullina, I.I. Shakhmaeva, I.I. Mavlyutova, T.I. Abdullin, Acta Nat. 4 (2012) 78–81.
[46] R.W. Davis, J.V. Volponi, H.D.T. Jones, B.J. Carvalho, H. Wu, S. Singh, Biotechnol. Bioeng. 109 (2012) 2503–2512.
[47] I. Herskowitz, Microbiol. Rev. 52 (1988) 536–553.
[48] A. Sanchis, A.P. Brown, M. Sancho, G. Martínez, J.L. Sebastián, S. Muñoz, J.M. Miranda, Bioelectromagnetics 28 (5) (2007) 393–401.
[49] J. Suehiro, J. Electrost. 57 (2) (2003) 157–168.
[50] J.L. Sebastian Franco, A. Sanchis Otero, J.R. Madronero, S.M. San Martin, Prog. Electromagn. Res.-Pier 134 (2013) 1–22.
[51] V.R.F. Matias, T.J. Beveridge, Mol. Microbiol. 56 (1) (2005) 240–251.
[52] J. Johari, Y. Hübner, J.C. Hull, J.W. Dale, M.P. Hughes, Phys. Med. Biol. 48 (14) (2003) (N193–8).
[53] J. Yang, Y. Huang, X. Wang, X.-B. Wang, F.F. Becker, P.R.C. Gascoyne, Biophys. J. 76 (6) (1999) 3307–3314.
[54] M.B. Sano, E.A. Henslee, E. Schmelz, R.V. Davalos, Electrophoresis 32 (22) (2011) 3164–3171.
[55] T. Müller, T. Schnelle, G. Fuhr, Polar Biol. 20 (5) (1998) 303–310.
[56] J.A. Riddick, W.B. Bunger, Organic Solvents: Physical Properties and Methods of Purification, Wiley, New York, 1989 (ISBN 978-0471-08467-9).
[57] O. Teschke, D.M. Soares, J.F.V. Filho, Appl. Phys. Lett. 103 (2013) 251608.